Characteristics of Nb/Al superconducting tunnel junctions fabricated using ozone gas

Masahiro Ukibe[†], Go Fujii, and Masataka Ohkubo

Nanoelectronics Research Institute (nano), National Institute of Advanced Industrial Science and Technology (AIST), 1-1-1 Umezono, Tsukuba, Ibaraki 305-8568, Japan

(Received 5 December 2014; revised manuscript received 28 April 2015; published online 3 August 2015)

To improve the energy resolution (ΔE) of Nb/Al superconducting tunnel junctions (STJs), an ozone (O_3) oxidation process has been developed to fabricate a thin defect-free tunnel barrier that simultaneously shows high critical current $J_C > 1000$ A/cm^2 and high normalized dynamic resistance $R_DA > 100$ MΩ · μm^2, where A is the size of the STJ. The 50-μm^2 STJs produced by O_3 exposure of 0.26 Pa·min with an indirect spray of O_3 gas, which is a much lower level of exposure than the O_2 exposure used in a conventional O_2 oxidation process, exhibit a maximum $J_C = 800$ A/cm^2 and a high $R_DA = 372$ MΩ · μm^2. The 100-pixel array of the 100-μm^2 STJs produced using the same O_3 oxidation conditions exhibits a constant leak current $I_{leak} = 14.9 \pm 3.2$ nA at a bias point around Δ/e (where e is half the energy gap of an STJ), and a high fabrication yield of 87%. Although the I_{leak} values are slightly larger than those of STJs produced using the conventional O_2 oxidation process, the STJ produced using O_3 oxidation shows a $\Delta E = 10$ eV for the C-Kα line, which is the best value of our Nb/Al STJ x-ray detectors.

Keywords: Nb/Al superconducting tunnel junctions, high critical current density, high energy resolution, ozone

PACS: 33.20.Kf, 33.70.Jg **DOI:** 10.1088/1674-1056/24/9/093301

1. Introduction

Fluorescence-yield x-ray absorption fine structure (FY-XAFS) spectroscopy is useful to characterize trace elements (dopants) in functional materials, such as next-generation compound semiconductor materials. In conventional XAFS measurements, semiconductor detectors are used to detect fluorescent x-rays. However, the energy-resolving power of the semiconductor detectors is not sufficient to clearly distinguish the K lines of light trace elements (e.g., boron and nitrogen) from the L lines of various elements, and the K lines of light elements in matrices in the energy range below about 3 keV. This insufficiency makes measurement of low-concentration dopants difficult. Superconducting tunnel junction (STJ) detectors are promising for XAFS measurements in the soft x-ray region, because of their high energy resolution and high sensitivity, both of which exceed those of semiconductor detectors.[1–3] In fact, our 100-pixel Nb/Al STJ array detectors had a mean energy resolution $\Delta E = 12$ eV for C-Kα (277 eV) photons. At this high-energy resolution, the XAFS spectra of 300 ppm nitrogen dopants in n-SiC samples were successfully obtained using a superconducting XAFS (SC-XAFS) apparatus.[4] With such high ΔE, it was possible to resolve the K lines of light trace elements, but it is difficult to achieve clear separation of the L lines of transition elements and the K lines of light elements. Therefore, further improvements in energy resolution are desirable. In general, the high critical current density (J_C) of STJs increases the x-ray signal output, and the low normalized dynamic resistance (R_DA) of STJs increases the circuit (system) noise when a charge preamplifier is used. Here, A is the size of the STJs. In a previous article,[5] it was shown that one of the possible ways to improve ΔE is to increase J_C to over 1000 A/cm^2, while maintaining a high R_DA of more than 100 MΩ · μm^2 (or a low leak current (I_{leak})) of the STJs. When Nb/Al STJs produced using the conventional fabrication process (an O_2 oxidation process) show high J_C values, they tend to exhibit low R_DA values (i.e., they have a large I_{leak}).[6] Motivated by these drawbacks, a new barrier formation process using ozone (O_3), which exhibits much stronger oxidation than O_2 gas, was introduced to fabricate a thin defect-free tunnel barrier. The dependence of J_C, I_{leak}, and R_D on the O_3 oxidation condition, which is represented by the product of the oxidant gas pressure (P) and the oxidation time (t), has been evaluated.[5] However, the STJs produced using the O_3 oxidation process exhibited extremely small J_C and I_{leak} values, which indicated a thick tunnel barrier. Even in the case of the lowest O_3 exposure of 0.72 Pa·min, which is a much lower level of exposure than the O_2 exposure applied in the conventional O_2 oxidation process (7.2×10^4 Pa·min), the J_C values were as small as 8 A/cm^2 and the I_{leak} value was lower than 50 pA, which was the lower limit of the measurement system. These results showed that the O_3 oxidation conditions must be optimized to realize a thin defect-free tunnel barrier and high J_C values of more than 1000 A/cm^2. In this study, the O_3 oxidation process was modified by changing the method of supplying the O_3 gas and the O_3 exposure. The performance of Nb/Al STJs

[†]Corresponding author. E-mail: ukibe-m@aist.go.jp

© 2015 Chinese Physical Society and IOP Publishing Ltd

made using the modified O_3 oxidation process was evaluated, and the dependences of J_C and R_D on the O_3 oxidation conditions, the fabrication yields, and the ΔE for soft x-rays were investigated.

2. Experiment

All STJs have an asymmetric layer structure. Here, this structure was Nb (300 nm)/Al (70 nm)/AlO_x/Al (70 nm)/Nb (50 nm). Two different types of STJ arrays were fabricated. The first was an 8-pixel array consisting of STJs with a size of 50×50 μm^2, which was used to measure the full current–voltage (I–V) curves. Because the critical current (I_C) of the superconducting Nb wirings (cross-section $\sim 1.2 \times 10^{-7}$ cm^2) used in the STJs was less than 0.1 Å,[7] it was necessary to use STJs with a size of 50×50 μm^2 to prevent the current flow in the Nb wirings from exceeding the I_C values of the Nb wirings when J_C was measured. The second was a 100-pixel array of STJs with a size of 100×100 μm^2, which was used to evaluate the x-ray detection performance. Figure 1 shows a top view of a Nb/Al STJ with a size of 50×50 μm^2. The STJs were fabricated using a conventional photolithographic technique, DC magnetron sputtering, a lift-off technique, reactive ion etching, and wet etching processes. These processes are described in detail in the literature.[8] The Nb/Al multilayer deposition and the tunnel barrier formation were performed by the same DC-sputtering apparatus, without breaking the vacuum, at room temperature. In the O_3 oxidation process, we reported in a previous article,[5] the oxidant gas was a mixture of gases prepared by diluting the O_3 (10%)/O_2 (90%) gas supplied by the O_3 generator with Ar gas, and this mixture was sprayed directly onto the surface of the bottom Al layer. However, the obtained relationship between J_C and Pt (the product of the oxidant gas pressure (P) and the oxidation time (t)) was $J_C \propto (Pt)^{-0.6}$, which was considered to be almost the same as the relationship of the low-J_C data described in Ref. [6] by taking into account the measurement error of the J_C values. This means that in the previous experiments, the influence of Al oxidation by O_2 gas during the total oxidation process was much larger than we first thought. Therefore, two alterations were made to the O_3 oxidation process. The first was that, to reduce the influence of O_2 gas as much as possible, one of the source gases of the oxidant gas was changed from a mixture of O_3 (10%)/O_2 (90%) to a mixture of O_3 (1.1%)/Ar (98.9%), which was supplied by the O_3 gas cylinder.[9] The second was that the oxidant gas was sprayed indirectly onto the surface of the bottom Al layer to make the gas composition of the oxidant gas more uniform and avoid the oxidation by dense clouds of O_3 gas. The properties of the junctions prepared using the modified O_3 oxidation process were compared with those of junctions prepared using O_2 oxidation. In the O_2 process, O_2 gas with 99.99% purity was used as the oxidant. The O_2 exposure was 7.2×10^4 Pa·min, which is the standard value used to fabricate STJ detectors for the soft x-ray region. The oxidation conditions used in the modified process are listed in Table 1.

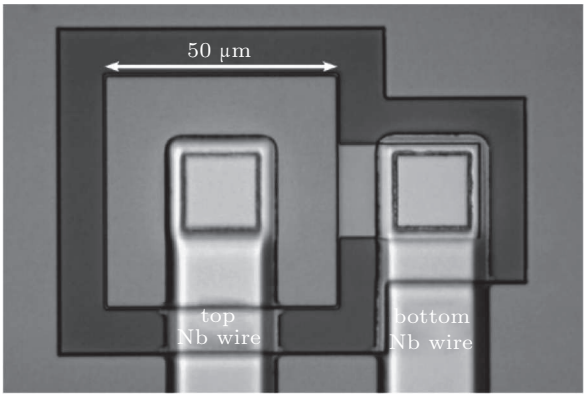


Fig. 1. Micrograph of an STJ used for the current–voltage (I–V) measurements.

Table 1. Summary of oxidation conditions.

Oxidant	O_2	O_3	O_3	O_3	O_3
Exposure/Pa·min	72000	264	26.4	2.64	0.264
Ratio to O_2 exposure	1	4×10^{-3}	4×10^{-4}	4×10^{-5}	4×10^{-6}

To create appropriate O_3 oxidation conditions, the O_3 exposure should be significantly lower than the exposure typically applied in O_2 processes, because oxidation by O_3 gas is much stronger than that by O_2 gas.[10] Measurement of the junction properties was performed using a cryogen-free ^{3}He cryostat with a base temperature of 0.31 K. The I–V characteristics were measured to evaluate J_C, the normal resistance (R_N), and R_D for all of the oxidation conditions. Note that J_C was measured in a zero field, and R_D was obtained using a linear approximation of the slope in the subgap region of the I–V curve in a magnetic field (B) of about 10 mT, which was applied along the diagonal direction of the STJs. The quality factor (Q) was then calculated by R_D/R_N. The x-ray detection performance (ΔE and the rise time (τ_r) of the x-ray signals) of the 100-pixel array was evaluated using the fluorescence x-rays generated by an x-ray tube. The x-ray tube consisted of a coniferous carbon nanostructure (CCNS) cathode[11] and a carbon compound target deposited on a pure Al plate. The fluorescent x-rays were generated by irradiating a carbon compound target with low-energy electrons (energies < 1 keV). The STJs were biased around Δ/e using constant bias currents. The magnetic field conditions were the same as those used to measure R_D, I_{leak} is defined as the subgap current value around Δ/e. The x-ray signals from the STJ array were processed using 100-channel charge-sensitive amplifiers and 100-channel FPGA-DSP based multi-channel analyzers.[12]

3. Result and discussion

3.1. Relationship between J_C, R_D, and O_3 exposure

Figure 2 shows the *I*–*V* curves of two STJs made using different oxidation conditions: O_2 exposure of 7.2×10^4 Pa·min and O_3 exposure of 0.264 Pa·min. Figures 2(a) and 2(c) show that $J_C = 220$ A/cm^2 and $R_DA = 2300$ MΩ · μm^2. The Q value of 2.4×10^6 is large enough for x-ray detection. In Figs. 2(b) and 2(d), J_C and R_DA are 800 A/cm^2 and 372 MΩ · μm^2, respectively. The Q value of 8.2×10^5 is large enough for x-ray detection. These values of the STJ made using the O_3 oxidation process are satisfactory. This is particularly true for the J_C value, which is approximately four times larger than that measured for the STJ fabricated using the conventional O_2 oxidation process. The J_C values are evaluated using the current values at the points of inflection outside the subgap regions of the *I*–*V* curves. It is assumed that the steep slopes observed around zero voltage in Figs. 2(a) and 2(b) are generated by the small resistances of about 0.01 Ω and 0.07 Ω, respectively, produced by the Au bonding pad. In the case of O_3 oxidation at 0.264 Pa·min, it is difficult to accurately ascertain the position of the inflection points outside the subgap region of the *I*–*V* curves because the resistance of the Au bonding pads is close to R_N, which lead to uncertainty in the J_C value. However, the results obtained using an O_3 exposure of 0.264 Pa·min indicate that it is possible to realize a thin tunnel barrier while maintaining a high R_D value by using an appropriate O_3 exposure. For 264 Pa·min O_3 oxidation, the I_{leak} value is less than 50 pA, which is the lower limit of our current measurement system. Therefore, all of the R_DA values of the STJs are larger than 20000 MΩ · μm^2. The properties of all of the STJs are shown in Table 2.

The J_C value measured for 0.264 Pa·min is the highest in our evaluation but is not significantly different from that measured for 2.64 Pa·min because of the above-mentioned uncertainty in the J_C value measured at 0.264 Pa·min. However, the overall relationship between J_C and O_3 exposure in the O_3 process using the indirect spray of the gas was considered to be valid, and the dependence of J_C on O_3 exposure (except for the case of 0.264 Pa·min) was $J_C \propto (Pt)^{-1.2}$, which is quite

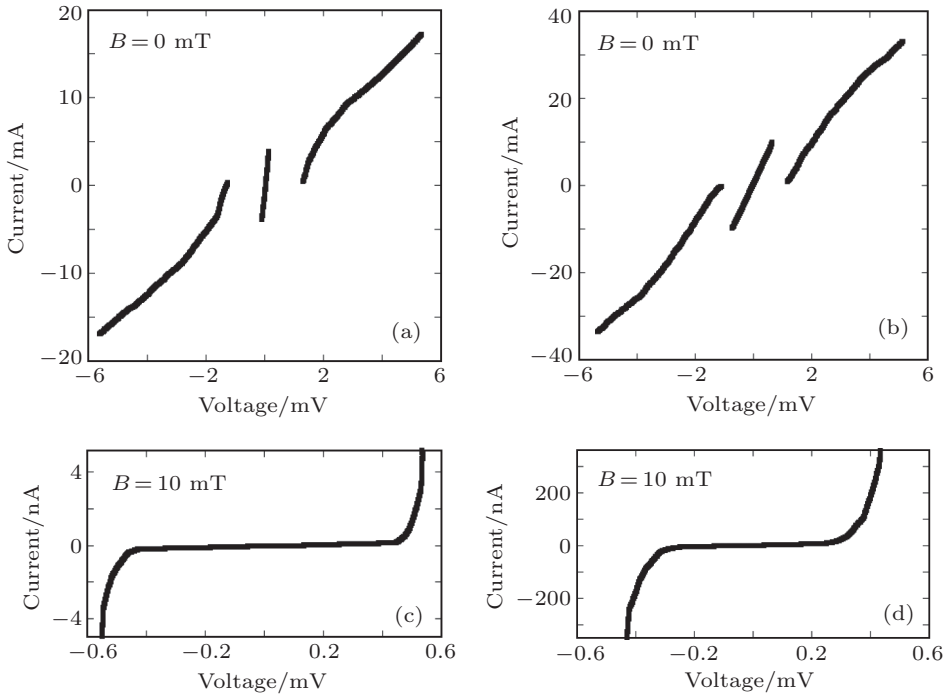


Fig. 2. *I*–*V* curves of two STJs made using different oxidation conditions: (a) and (c) O_2 exposure of 7.2×10^4 Pa·min, and (b) and (d) O_3 oxidation at 0.264 Pa·min. The J_C and R_D values were measured at $B = 0$ mT ((a) and (b)) and $B = 10$ mT ((c) and (d)), respectively.

Table 2. Summary of junction properties.

Oxidant	O_2	O_3	O_3	O_3	O_3
Exposure/Pa·min	72000	264	26.4	2.64	0.264
J_C/A·cm^{-2}	228 ± 9	2.5 ± 0.17	118 ± 3	720 ± 28	800 ± 28
R_DA/MΩ · μm^2	2368 ± 118	> 20000	4470 ± 343	585 ± 91	372 ± 26
$Q(R_D/R_N)/10^5$	24 ± 1	> 0.27	27 ± 2	13 ± 2	8.5 ± 0.6

different to that for the low-J_C data described in Ref. [6]. This indicates that the Al oxidation process by O_3 gas is different from that by O_2 gas. The relationship between J_C and O_3 exposure in the O_3 process is plotted in Fig. 3 for the processes performed using indirect and direct spray of the gas.[5]

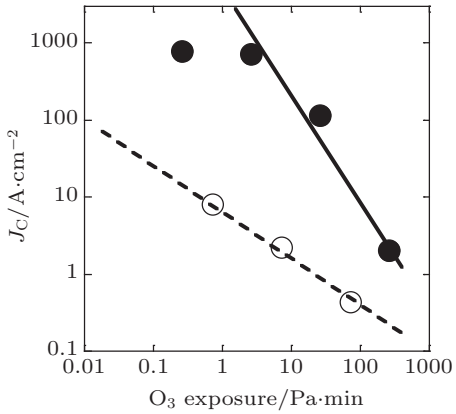


Fig. 3. Relationship between J_C and O_3 exposure in the O_3 process for indirect (solid circles) and direct (open circles) spray of the gas. The solid and dashed lines are fit to the data for indirect and direct spray of the gas, and indicate the dependencies $J_C \propto (Pt)^{-1.2}$ and $J_C \propto (Pt)^{-0.6}$, respectively.

It was found that an indirect spray of O_3 was very effective in reducing the tunnel barrier thickness, which led to the increase in J_C. The best O_3 oxidation conditions in our evaluation were an O_3 exposure of 0.264 Pa·min using an indirect spray of gas. Under these conditions, the highest J_C value of 800 ± 28 A/cm^2 was achieved.

3.2. X-ray detection performance of STJs fabricated under the best O_3 oxidation conditions

The x-ray detection performance of the STJs fabricated under the best O_3 oxidation conditions was evaluated. The size of these STJs was 100×100 μm^2. 87 out of 100 STJs in the array detector exhibited $I_{leak} < 30$ nA, i.e., $R_DA > 100$ MΩ · μm^2, which means that the fabrication yield was 87%. These STJs were good enough to detect x-ray photons. The average and standard deviations of the leakage current were 14.9 nA and 3.2 nA, respectively. The excellent uniformity of the leakage currents allowed each STJ in the array detector to be operated at a uniform bias current. Figure 4 shows an *I*–*V* curve of an STJ in the 100-pixel array at $B = 10$ mT. The fluorescent x-rays from the x-ray tube were measured, and a typical x-ray signal pulse is shown in Fig. 5.

The rise time (τ_r) of the x-ray signal pulse was 21 μs, which is approximately twice as long as that of conventional STJs (∼ 12 μs). This increase in τ_r occurred because the frequency of the quasiparticle tunneling increased. This was the result of the increased tunneling provability, which was itself a result of the high J_C.[13,14] A fluorescent x-ray spectrum is shown in Fig. 6.

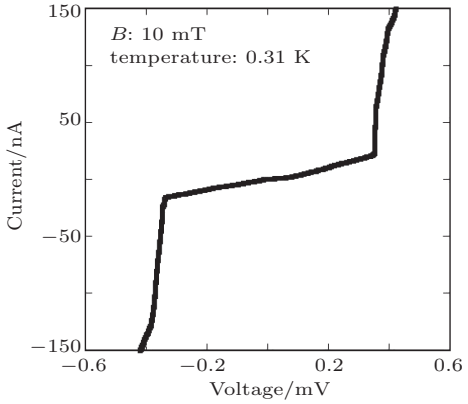


Fig. 4. *I*–*V* curve for an STJ of the 100-pixel array made using an O_3 exposure of 0.264 Pa·min at $B = 10$ mT.

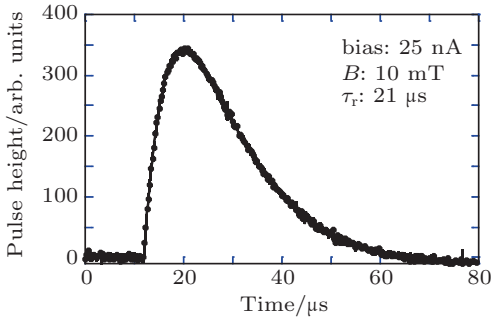


Fig. 5. Typical x-ray signal pulse obtained using an STJ in the array made using an O_3 exposure of 0.264 Pa·min.

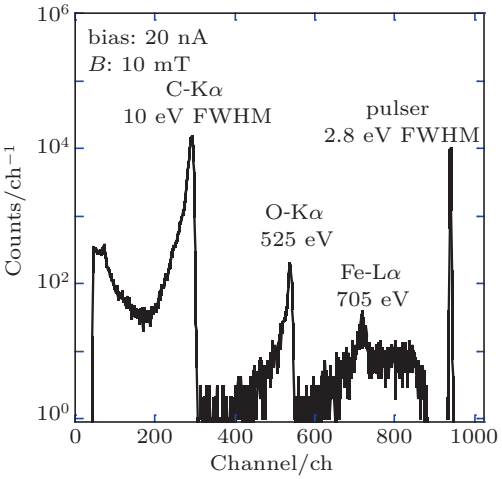


Fig. 6. X-ray spectrum of an STJ in the array for measuring fluorescent x-rays from the x-ray tube. The C-Kα, O-Kα, and Fe-Lα x-rays in the spectrum were emitted from a carbon compound target, oxide in the carbon compound target, and iron in the Al plate, respectively. The x-ray signals from approximately 700–900 ch correspond to bremsstrahlung x-ray photons generated in the Al plate of the target.

The energy resolution of C-Kα and the circuit noise were 10 and 2.8 eV (FWHM), respectively. The O-Kα and Fe-Lα x-rays shown in Fig. 6 were emitted from oxide in the carbon compound target and iron in the Al plate of the target, respectively. The x-ray signals from approximately 700–900 ch in Fig. 6 correspond to bremsstrahlung x-ray photons generated in the Al plate of the target. The ΔE measured for the C-Kα

line is the best ΔE value measured for our Nb/Al STJs to date. This value is higher than that for silicon drift detectors, which are the semiconductor detectors that currently give the best ΔE value in the soft x-ray region.[15] We therefore succeeded in realizing an STJ array detector with high J_C and good energy resolution using the O_3 oxidation process.

4. Conclusion

To improve the ΔE of Nb/Al STJs, the O_3 oxidation process was modified to fabricate a thin defect-free tunnel barrier that simultaneously showed a high critical current $J_C >$ 1000 A/cm^2 and a high normalized dynamic resistance $R_DA >$ 100 M$\Omega \cdot \mu$m^2. The 50-μm^2 STJs produced using O_3 oxidation of 0.26 Pa·min with the indirect spray of the gas, which is a much lower level of exposure than the O_2 exposure used in the conventional O_2 oxidation process, exhibited a maximum $J_C = 800$ A/cm^2 and a high $R_DA = 372$ M$\Omega \cdot \mu$m^2. The 100-pixel array of 100-μm^2 STJs made using the same O_3 oxidation conditions showed a constant $I_{leak} = 14.9 \pm 3.2$ nA at the bias point, and a high fabrication yield of 87%. Although the I_{leak} values were slightly larger than those of STJ arrays produced using the conventional O_2 oxidation process, the STJ produced using O_3 oxidization showed a $\Delta E = 10$ eV for the C-Kα line, which is the best value yet shown for our Nb/Al STJs.

Acknowledgments

The authors thank S. Shiki for his help with the experiments, and T. Adachi and the clean room members of analog-digital superconductivity (CRAVITY) for performing the STJ fabrication.

References

[1] Ukibe M, Shiki S, Kitajima Y and Ohkubo M 2012 *Jpn. J. Appl. Phys.* **51** 010115
[2] Fons P, Tampo H V. Kolobov A, Ohkubo M, Niki S, Tominaga J, Carboni R, Boscherini F and Friedrich S 2006 *Phys. Rev. Lett.* **96** 045504
[3] Friedrich S, Funk T, Drury O, Labov S E and Cramer S P 2002 *Rev. Sci. Instrum.* **73** 1629
[4] Ohkubo M, Shiki S, Ukibe M, Matsubayashi N, Kitajima Y and Nagamachi S 2012 *Sci. Rep.* **2** 831
[5] Ukibe M, Fujii G and Ohkubo M 2014 *J. Low Temp. Phys.* **176** 142
[6] Miller R E, Mallison W H, Kleinsasser A W, Delin K A and Macedo E M 1993 *Appl. Phys. Lett.* **63** 1423
[7] Youssef A E, Švindrych Z, Hadač J and Jansů Z 2007 *WDS's* 07 *Proceedings* (Part III) 48
[8] Ukibe M, Kushino A, Chen Y and Ohkubo M 2007 *X-ray Spectr.* **36** 260
[9] http://www.iwatani.co.jp/jpn/div/ing_wem/ele_gas/cylinder/main.html
[10] Horvath M, Bilitzky L and Huttner J 1985 *Ozone* (New York: Elsevier)
[11] Kato H, O'Rourke B E and Suzuki R 2014 *JJAP Conf. Proc.* 2 011302
[12] Shiki S, Ukibe M, Kitajima Y and Ohkubo M 2012 *J. Low Temp. Phys.* **167** 748
[13] Mears C A, Labov S E and Barfknecht A T 1993 *Appl. Phys. Lett.* **63** 2961
[14] Goldie D J, Brink P L, Patel C, Booth N E and Salmon G L 1994 *Appl. Phys. Lett.* **64** 3169
[15] Schlosser D M, Lechner P, Luts G, Niculae A, Soltau H, Struder L, Eckhardt E, Hermenau K, Schaller G, Schopper G, Jaritschin O, Liebel A, Simsek A, Fiorini C and Longini A 2010 *Nucl. Instrum. Methods Phys. Res., Sect. A* **624** 270